TISSUE ENGINEERING: Part A
Volume 15, Number 4, 2009

DOI: 10.1089/ten.tea.2008.0109

Chondrogenic Differentiation of Human Mesenchymal Stem Cells on Oriented Nanofibrous Scaffolds: Engineering the Superficial Zone of Articular Cartilage

Joel K. Wise,[1] Alexander L. Yarin,[2] Constantine M. Megaridis,[2] and Michael Cho[1]

Cell differentiation, adhesion, and orientation are known to influence the functionality of both natural and engineered tissues, such as articular cartilage. Several attempts have been devised to regulate these important cellular behaviors, including application of inexpensive but efficient electrospinning that can produce patterned extracellular matrix (ECM) features. Electrospun and oriented polycaprolactone (PCL) scaffolds (500 or 3000 nm fiber diameter) were created, and human mesenchymal stem cells (hMSCs) were cultured on these scaffolds. Cell viability, morphology, and orientation on the fibrous scaffolds were quantitatively determined as a function of time. While the fiber-guided initial cell orientation was maintained even after 5 weeks, cells cultured in the chondrogenic media proliferated and differentiated into the chondrogenic lineage, suggesting that cell orientation is controlled by the physical cues and minimally influenced by the soluble factors. Based on assessment by the chondrogenic markers, use of the nanofibrous scaffold (500 nm) appears to enhance the chondrogenic differentiation. These findings indicate that hMSCs seeded on a controllable PCL scaffold may lead to an alternate methodology to mimic the cell and ECM organization that is found, for example, in the superficial zone of articular cartilage.

Introduction

Articular or hyaline cartilage tissue is comprised of at least four distinct zones, each with a specific cell and extracellular matrix (ECM) organization or orientation.[1–7] The four zones—known as superficial/tangential, intermediate/transitional, deep/radial, and calcified zone—naturally function collectively to provide the low-friction, wear-resistant, load-bearing tissue on the end of bones in synovial joints. The specific cell and ECM organization within each cartilage zone can be attributed to developmental history and to the mechanical forces to which each zone is subjected, thereby supporting the overall functionality of articular cartilage tissue.[8–13]

Osteoarthritis, trauma, aging, and developmental disorders commonly result in degeneration or even loss of hyaline cartilage, which has no or little ability of self-repair due to the lack of vasculature. It has been shown that early stages of osteoarthritis and age-associated weakening can lead to alterations of the thin surface or superficial zone of articular cartilage (~200 μm in depth), and its damage.[6,10] Degeneration or remodeling of the dense collagenous matrix of the superficial zone in turn causes changes in the mechanical behavior of the tissue, as well as release of collagen molecules into the synovial fluid, stimulating an immune response.[5,6]

The superficial zone of natural functioning articular cartilage consists of primarily flattened ellipsoidal-like chondrocytes and a very polarized dense organization of nanoscale collagen type II fibrils (approximately 20 nm diameter), which are oriented parallel to the plane of the articular surface.[1–7] Compared to the other zones of articular cartilage, the superficial zone consists of the highest concentration of collagen and the lowest concentration of proteoglycans, such as aggrecan.[2,3,5,6] Due to the alignment of chondrocytes and collagen type II fibrils, the thin superficial zone has the greatest tensile strength found in articular cartilage, which is crucial for resisting shear and tensile forces from the articulating surfaces.[2,3] Additionally, the superficial zone is also important for some compressive strength of the cartilage tissue and also in the isolation of cartilage from the immune system by forming an effective seal at the joint surface.[2]

Similar to chondrocytes in the superficial zone of natural articular cartilage, cells and ECM fibrils in most natural tissues are not random, but exhibit well-defined patterns and specific spatial orientation. Recent findings demonstrated that oriented nanofibrous scaffolds have the potential for engineering blood vessels,[14] neural tissue,[15] and ligament tissue.[16] Further, it has also been shown that cell adhesion and

Departments of [1]Bioengineering and [2]Mechanical and Industrial Engineering, University of Illinois at Chicago, Chicago, Illinois.

proliferation is significantly improved on oriented nanofibrous scaffolds.[14] The present study is therefore focused on engineering a tissue-like construct that will mimic the superficial zone of articular cartilage using bone marrow–derived human mesenchymal stem cells (hMSCs) and electrospun biocompatible polycaprolactone (PCL) scaffolds. Although several studies have been published to demonstrate that hMSCs or chondrocytes can be cultured on oriented electrospun nanofibrous scaffolds,[17,18] attempts to specifically engineer the superficial zone of the articular cartilage are currently lacking. Here we report that alignment and chondrogenic differentiation of hMSCs cultured on oriented electrospun PCL scaffolds are feasible and relatively easy to implement. hMSCs seeded on the aligned PCL scaffolds maintained the cell orientation at least up to 5 weeks; such fiber-guided orientation, but not differentiation, was independent of the fiber size. For example, chondrogenic differentiation was facilitated when cells were seeded on a nanofibrous scaffold (~500 nm diameter). It appears that stem cell–based therapeutic application and tissue engineering may be enhanced by physical approaches such as the one presented herein to control the microenvironment and therefore promote stem cell differentiation.

Materials and Methods

Electrospinning of PCL fibrous scaffolds

Oriented PCL scaffolds were produced using the electrospinning method as described previously.[19–21] All electrospun polymer fibrous scaffolds were made from PCL with molecular weight of 80 kDa (Sigma-Aldrich, St. Louis, MO). Fibers were electrospun from a 10% PCL solution dissolved in methylene chloride/dimethylformamide with a ratio of 75/25 (vol.). The oriented scaffolds were produced by collecting the fibers on a narrow strip mounted over the sharp edge of a rotating disk,[20–22] resulting in a fibrous scaffold with a clearly defined orientation in the direction of the disk rotation. The polymer solution was electrospun from a 5 mL syringe with a hypodermic needle (inner diameter 0.1 mm) and at a flow rate of 1 mL/h. A copper electrode was placed in the polymer solution, and the latter was electrospun onto the sharp edge of an electrically grounded collector (rotating disk). The strength of the electric field was 1.1 kV/cm, and the linear speed of the edge of the disk collector was 10 m/s. All experiments were performed at ambient temperature (~25°C) in air with 40% relative humidity. A scanning electron microscope (SEM; Hitachi S-3000N, Tokyo, Japan) was used to obtain images of each type of fibrous PCL scaffold. This instrument has a tungsten electron source and is capable of imaging specimens in variable pressures ranging from 1 to 270 Pa. Under variable pressure, nonconducting specimens can be imaged without coating of conductive film. The accelerating voltage can be varied over the range 0.3–30 kV with a resolution of 5 nm at 25 kV. Fiber diameters were estimated using an image processor (MetaMorph; Molecular Device, Downingtown, PA). Additionally, to serve as PCL control samples for comparison of cell orientation and viability, a nonelectrospun randomly porous PCL film was produced by pouring a thin layer of 10% PCL solution over a flat surface (~1 mm thick), which was then allowed to dry. As the solvent evaporated, a randomly porous and thin polymer film was produced and removed from the substrate for subsequent cell culture experiments.

Human mesenchymal stem cell culture and cell seeding on PCL scaffolds

hMSCs were obtained from the Center for Gene Therapy (Tulane University, New Orleans, LA). Cells were cultured in complete growth media consisting of Dulbecco's modified Eagle's medium (DMEM; Invitrogen, Carlsbad, CA) supplemented with 15% fetal bovine serum (FBS; Atlanta Biologicals, Lawrenceville, GA), 2 mM L-glutamine (Sigma), 1% antibiotics and antimycotics (final concentration: penicillin 100 units/mL, streptomycin 100 μg/mL, and amphotericin B 0.25 μg/mL; Sigma). Cells at passage 3 were used. The electrospun PCL fibers were cut (~2 cm^2) and inserted into the 24-well plates for cell culture. The scaffolds were immersed in 70% ethanol for 1 h, placed in a vacuum chamber for 3 days to remove any residual organic solvent, and sterilized under UV light for 6 h on each side. To promote protein adsorption and cell attachment, the scaffolds were immersed in complete culture media for 48 h prior to cell seeding. To seed hMSCs onto the PCL fibrous scaffolds and PCL film (i.e., control scaffold), cells were pipetted directly onto the scaffolds at a density of 6×10^4 cells/cm^2 and cultured in complete growth media for 24 h. For chondrogenesis, the media was replaced with a chondrogenic differentiation media (4500 mg/L D-glucose, L-glutamine, and 110 mg/L sodium pyruvate; Invitrogen) that was supplemented with 10 ng/mL TGF-β_1 (Research Diagnostics, Concord, MA), 100 nM dexamethasone (Sigma), 50 μg/mL ascorbate 2-phosphate (Sigma), 40 μg/mL proline (Sigma), and 1% liquid media supplement (ITS + 1; Sigma). Either complete growth media or chondrogenic differentiation media was replaced every 2–3 days.

Fluorescent cell viability and orientation analysis

Cell viability and orientation analysis were performed 4 days after initial cell seeding onto scaffolds, and subsequently at 7-, 21-, and 35-day time points. For fluorescence cell viability, cells were stained using a live-dead cell viability assay (Molecular Probes, Carlsbad, CA). Images were taken from at least three different and randomly chosen views on each sample at the different culture time points of 4, 7, 21, and 35 days. Using an image processor (MetaMorph; Universal Imaging, West Chester, PA), the orientation of each cell was determined by identifying its major axis with respect to the horizontal axis. Because the cells were stained with the CMTMR cell tracker (Molecular Probes), the image processor efficiently utilized significant differences in the fluorescence intensity between the CMTMR-loaded cells and background to identify cell boundaries and the major and minor axes of the cell.

Sulfated glycosaminoglycan and DNA extraction and quantitation

Samples were digested in 100 μL solution of 300 μg/mL papain in 20 mM PBS, pH 6.8, 5 mM EDTA, 2 mM DTT at 60°C for 18 h (all reagents from Sigma-Aldrich). For total sGAG quantitation, 50 μL of the extract for each sample was used with the Blyscan™ Sulfated Glycosaminoglycan (sGAG) Assay Kit (Biocolor, County Autrim, UK). Briefly, 1 mL of 1,9-dimethyl-methylene blue dye reagent was added to 50 μL of the extract and allowed to react for 30 min. The blue dye binds to sGAG and forms a purple dye–sGAG precipitate, which

was separated from the unbound dye solution by centrifugation at 10,000 *g*. To recover the sGAG-bound dye from the resulting pellet, 200 μL of dissociation reagent was added. Absorbance of dye from sGAG samples, chondroitin 4-sulfate standards, and blanks were quantified spectrophotometrically with a filter (655 ± 5 nm) on a microplate reader (Bio-Rad Laboratories, Hercules, CA). For total DNA analysis, a fluorescent DNA Quantitation Kit (Bio-Rad Laboratories) containing Hoechst 33258, calf thymus DNA standard, and 10× TEN Assay Buffer was used. Briefly, 20 μL from the remaining 50 μL of the DNA/sGAG extract was added to 80 μL of 1 μg/mL Hoechst 33258 dye (in 10× TEN Assay Buffer). Different volumes of 10 μg/mL calf thymus DNA were added to 80 μL of 1 μg/mL Hoechst 33258 dye to obtain a standard calibration curve (ranging from 20 to 100 ng DNA) for converting relative fluorescence units into nanograms of DNA for samples. The fluorescence of the Hoechst 33258–DNA complex in the samples, standards, and blanks was detected at excitation/emission wavelengths of 360 nm/460 nm using a microplate spectrofluorometer (Molecular Devices, Sunnyvale, CA).

RNA extractions and quantitative real-time PCR for chondrogenic gene expression

Using quantitative real-time PCR, the mRNA expression of cartilage-specific genes, such as collagen type II and aggrecan, were analyzed from samples. RNA was isolated from the samples by using TRIzol reagent (Invitrogen) according to the manufacturer's instructions. The concentration and integrity of RNA were estimated spectrophotometrically with a Beckman DU-600 Spectrophotometer at $A_{260/280}$. The RNA samples were reverse transcribed into first-strand cDNA using the SuperScript III First-Strand Synthesis SuperMix Kit for two-step qRT-PCR (Invitrogen). Gene-specific amplicons from the cDNA of each sample were amplified and quantitatively measured by real-time PCR using SYBR Green qPCR SuperMix-UDG with ROX kit (Invitrogen) and an ABI Prism 7900HT Sequence Detection System (Applied Biosystems, Foster City, CA). Reactions were carried out at 50°C for 2 min, 95°C for 2 min, 50 cycles of 95°C for 15 s, and 60°C for 30 s, followed by a melting curve analysis. Samples were loaded in duplicate in 96-well plate with a final volume of 25 μL, containing cDNA generated from 1 μg RNA and mixed with SYBR Green Mix and cartilage-specific primers. These gene primers were purchased from Sigma-Aldrich (Genosys). The cartilage-specific oligonucleotide primers used were aggrecan, 5′-TGAGGAGGGCTGGAACAAGTA-CC-3′ and 5′-GGAGGTGGTAATTGCAGGGAACA-3′, and collagen type II, 5′-CAGGTCAAGAT-GGTC-3′ and 5′-TTCAGCACCTGT CTCACCA-3′. The housekeeping gene Glyceraldehyde-3-phosphate dehydrogenase (GAPDH), 5′-GGGCTGCTTTT AACTCTG-GT-3′ and 5′-GCAGGTTTTTCTAGACGG-3′, was used as an endogenous reference for RNA loading of samples. Fold induction and expression levels for each target gene were calculated using the comparative C_t method, which can be expressed as $2^{-([\Delta Ct,\ test]-[\Delta Ct,\ control])}$, where C_t was threshold cycle, and $\Delta C_{t,\ test}$ and $\Delta C_{t,\ control}$ presented the difference between C_t target and C_t reference of test samples and control samples.

Statistical analysis

Data were expressed as the mean ± standard deviation (SD). The cell angle distributions on each scaffold sample were statistically analyzed with Student's two-tailed *t* test, with $p > 0.05$ being considered not statistically significant. For PCL film scaffolds used as control, there was no preferential direction of cell orientation and the average cell angle values were not determined.

Results

Electrospun PCL fibrous scaffolds

SEM imaging was first performed to observe the structural morphology of fibers in each of the three electrospun PCL scaffolds of oriented fibers that have an average fiber diameter of approximately 500 nm (492 ± 120 nm; Fig. 1A) and 3000 nm

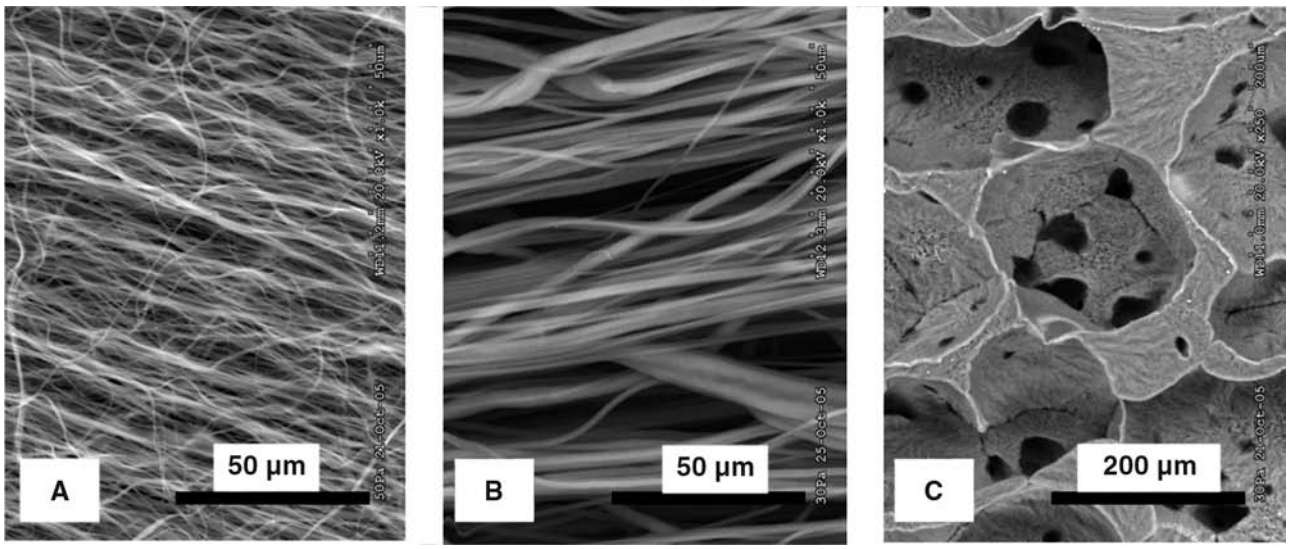

FIG. 1. SEM images of oriented electrospun PCL fibrous scaffolds. The average fiber diameter was estimated using an image processor: (**A**) 500 nm; (**B**) 3000 nm. (**C**) shows nonelectrospun porous PCL film.

(2796 ± 845 nm; Fig. 1B). The majority of the fibers in the oriented fibrous scaffolds were aligned with respect to each other. The nonelectrospun PCL film (Fig. 1C), which served as a control scaffold, consisted of a randomly porous surface with average pore sizes of approximately 100–250 μm. Based on the SEM images, all electrospun PCL scaffolds demonstrated interconnected pores that are likely suitable for cell viability and proliferation. In addition, the oriented fibrous network density could be sufficient to provide a suitable substrate for cell adhesion and spreading.

Cell viability and orientation on PCL scaffolds

hMSCs seeded (6×10^4 cells/cm^2) on the PCL fibrous scaffolds were imaged using laser scanning confocal microscopy to determine the effect of electrospun PCL fiber orientation on cell alignment. To test the cell viability and fluorescently visualize the cell morphology, cells were loaded with calcein fluorophore (Molecular Probes). For example, as shown in Figure 2, hMSCs seeded on the nanofibrous (500 nm; Fig. 2A) or microfibrous (3000 nm; Fig. 2B) scaffolds and incubated in the normal growth media showed a preferential orientation along the direction of the fibers. To quantify the extent of cell orientation, at least 75 cells from each sample were selected randomly and their orientation with respect to the reference (i.e., horizontal axis) was determined using the MetaMorph image processor. Based on this analysis, a histogram of the cell orientation angle distribution was created and displayed next to the fluorescent image in Figure 2. As expected, cells seeded on the nonelectrospun PCL film showed no preferred direction of orientation, which is confirmed by the corresponding histogram of the orientation angles (Fig. 2C). When cells were incubated in the chondrogenic media, similar results on cell orientation were observed on the nano- or microfibrous scaffolds (Fig. 2D and E, respectively), and again virtually no prevailing cell orientation on the PCL film (Fig. 2F) was found. The chondrogenic factors do not appear to alter significantly the cell orientation guided by the PCL fibers. However, one

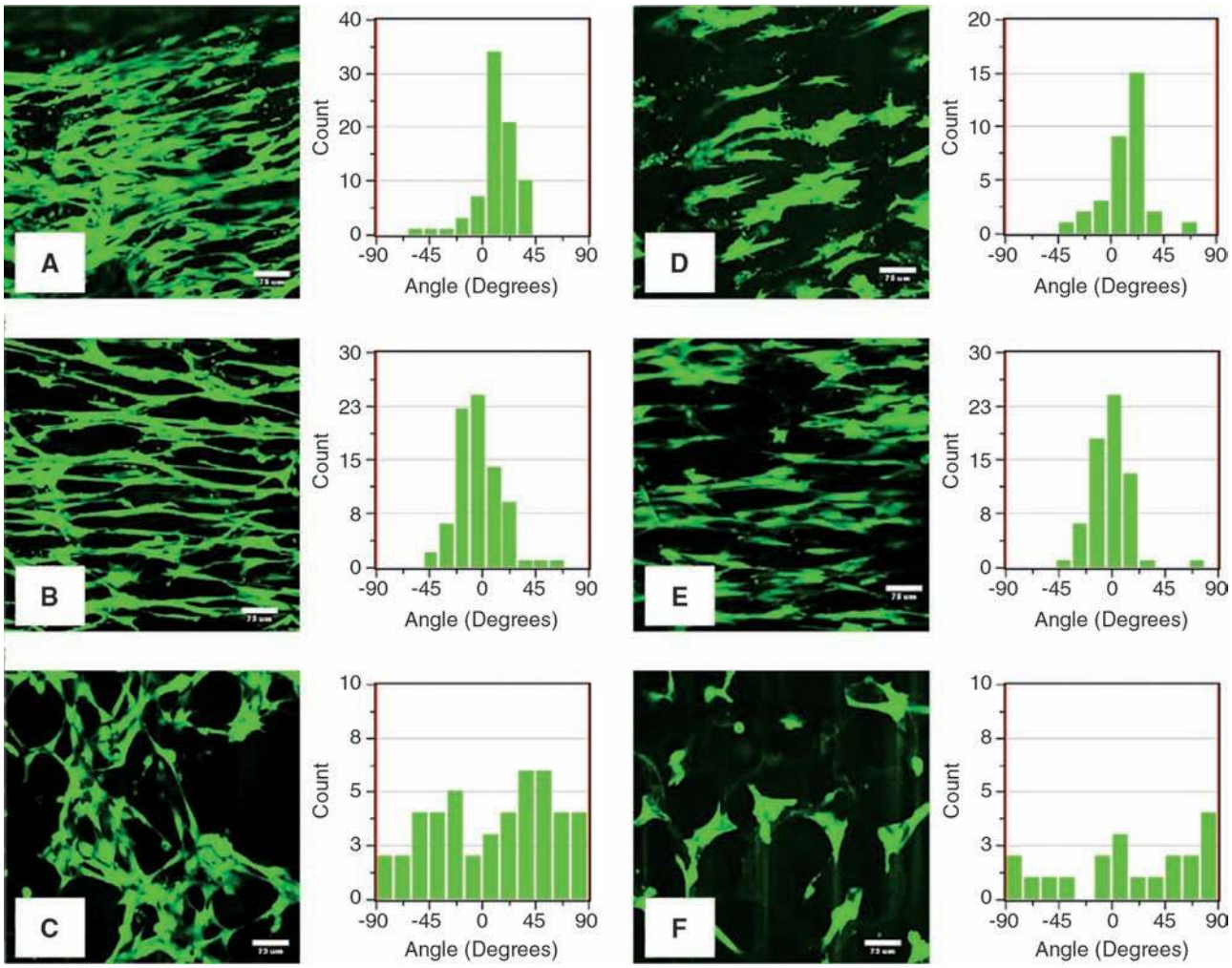

FIG. 2. Quantitative assessment of fiber-guided cell orientation. Viable hMSCs (green) cultured in normal growth media for 4 days on electrospun oriented PCL fibrous scaffolds of average fiber diameters of 500 nm (**A**), and 3000 nm (**B**), as well as on nonelectrospun PCL film (**C**). Images of viable hMSCs cultured in the chondrogenic differentiation media for 4 days on electrospun oriented PCL scaffolds of average fiber diameters of 500 nm (**D**) and 3000 nm (**E**), and on nonelectrospun PCL film (**F**). Adjacent to each cell image are histograms representing the corresponding distributions of cell orientation angles with respect to the horizontal axis. Approximately 80 cells (except those on the PCL film) were used to construct the histograms. Scale bar denotes 75 μm. Color images available online at www.liebertonline.com/ten.

noticeable difference was that the cells in the chondrogenic media were not as elongated as those found in the normal growth media, suggesting that cell shape was likely affected by the chondrogenic factors. In addition, cells seeded on the microfibrous scaffolds appear to be better oriented than those on the nanofibrous scaffolds.

The efficacy of oriented PCL fibrous scaffolds in maintaining a long-term cell alignment of hMSCs was quantitatively analyzed over a period of 5 weeks either in growth media or in chondrogenic media. Although visual inspections of the histograms indicate that the majority of cells on the nano- or microfibrous scaffolds are indeed oriented along a dominant direction (that of the underlying fibers), the cell orientation as a function of time is assessed by calculating the standard distribution of the cell orientation angle. While the oriented cells would have a minimal standard deviation (SD), the randomly distributed cells are expected to show large SDs. hMSCs seeded on the PCL scaffolds and placed in the normal growth media maintained their orientation for at least 5 weeks (Fig. 3A), and this fiber-guided cell orientation was minimally influenced by the chondrogenic factors. hMSCs aligned along the fibers and undergoing biochemically directed chondrogenic differentiation also maintained their orientation (Fig. 3B). For example, the SD of the cell angles for hMSCs cultured on PCL nanofibers for 4 days in the chondrogenic media was 22° and did not vary substantially over the 5-week differentiation period. In comparison, hMSCs seeded on the PCL film in the chondrogenic media showed an SD of the cell orientation angle as large as 60°. hMSCs cultured on the fibrous PCL scaffolds demonstrated consistent alignment for initial and long-term culture, independent of fiber diameter and culture media condition.

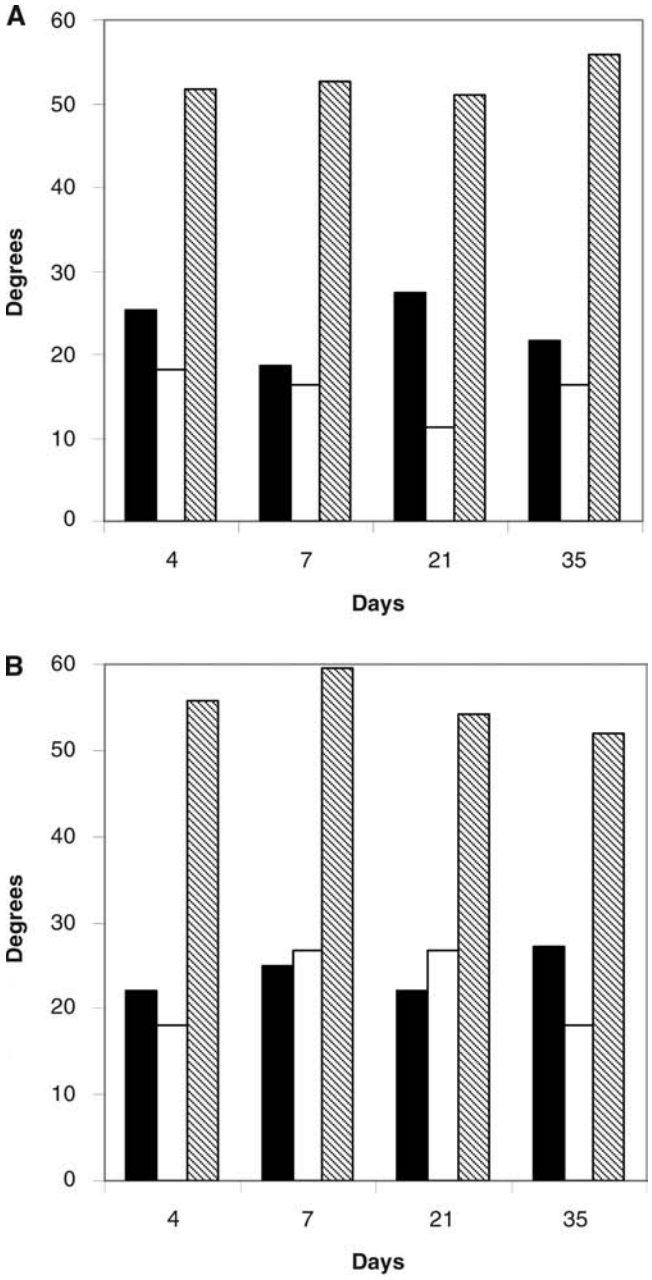

FIG. 3. Time-dependent changes of the SD of cell angle measurements. Cultured either in normal growth media (**A**) or chondrogenic differentiation media (**B**), the cell angle measurements were performed at day 4, 7, 21, and 35. SDs of the measurements were calculated for cells aligned on the nanofibrous (black bars), microfibrous (open bars) scaffolds, and on the non-electrospun PCL film (hatched bars). The fiber-guided initial cell alignment was essentially maintained for at least 35 days.

Cell proliferation and chondrogenic differentiation

Total DNA amounts were next analyzed by a DNA assay kit to measure the cell proliferation. Figure 4 shows the average of total DNA amounts measured at days 1 and 35 from hMSCs cultured in the growth or chondrogenic media and seeded on the electrospun oriented PCL fibrous scaffolds of fiber diameter 500 nm (Fig. 4A), 3000 nm (Fig. 4B), and the nonelectrospun PCL film (Fig. 4C). The differences between the total DNA amounts from hMSCs on all scaffold samples and in either culture media condition were found to be not statistically significant, although a slight decrease was observed for the cells seeded on the PCL film for 5 weeks (Fig. 4C). Therefore, the PCL fiber size does not appear to affect the cell proliferation. Using sGAG as a chondrogenic differentiation marker, the total sGAG amounts synthesized at days 1 and 35 were quantified using a GAG assay kit. Figure 5 summarizes the ratio of the average amounts of total sGAG measured from hMSCs cultured in the growth or chondrogenic media and seeded on the PCL fibrous scaffolds of 500 nm fibers (Fig. 5A), 3000 nm fibers (Fig. 5B), and on the nonelectrospun PCL film (Fig. 5C). Results from day 1 showed that all samples, whether cultured in the growth or chondrogenic media, had a baseline value of approximately 1 μg sGAG/μg DNA. As expected, following a 35-day culture, samples cultured in the chondrogenic media showed a significant increase in the GAG content. Such an increase is clearly noticeable in hMSCs seeded on the nanofibrous PCL scaffold (Fig. 5A). While the GAG content measured from the cells seeded on the nanofibrous scaffold but cultured in the growth media did not show substantial increase from day 1 to 35, approximately a fivefold rise in the GAG content was found when the cells were incubated in the chondrogenic media. In contrast, although hMSCs seeded on the microfibrous scaffold and cultured in chondrogenic media also demonstrated a large increase in the GAG content by day 35, the relative increase when compared

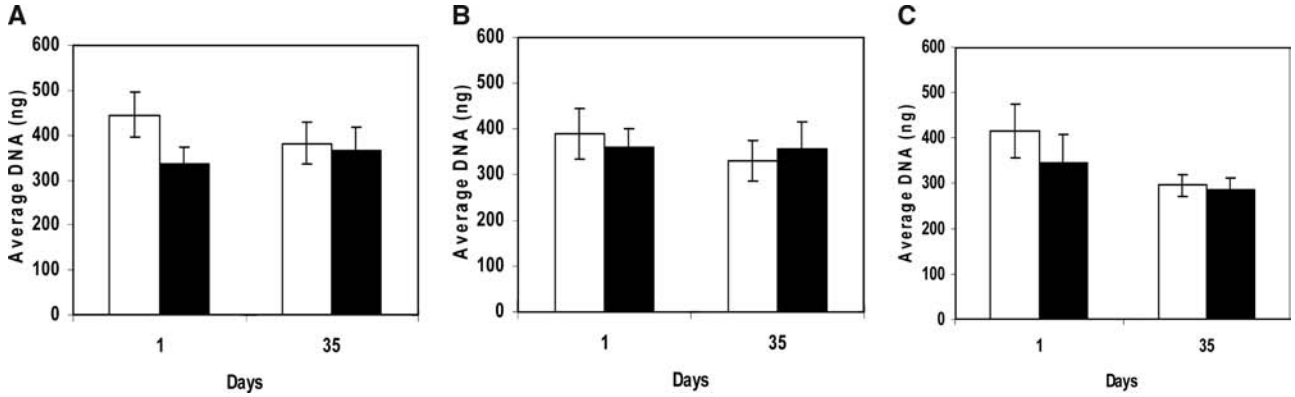

FIG. 4. Total DNA amount measured at days 1 and 35. hMSCs cultured in growth media (open bars) or chondrogenic differentiation media (black bars) on electrospun oriented PCL fibrous scaffolds of average fiber diameters of 500 nm (**A**) and 3000 nm (**B**), as well as on nonelectrospun PCL film (**C**). Results represent the mean ± SEM of three independent experiments.

to hMSCs cultured in the growth media was about twofold (Fig. 5B). Based on the GAG content measurements, only the nanofibrous scaffold suppressed the GAG expression in the absence of the chondrogenic factors. Finally, we used quantitative real-time PCR to measure the gene expressions of collagen type II and aggrecan (e.g., two additional chondrogenic markers). As shown in Figure 6, the expression of collagen type II was upregulated in all samples cultured in the chondrogenic media for 35 days, especially on the nanofibrous PCL scaffold (500 nm), where a nearly 30-fold increase was measured. The aggrecan gene expression was also measured, and the cells seeded on the nanofibrous scaffold resulted in about a fivefold rise. Interestingly, while cells seeded on the control PCL film also expressed an elevated level of the aggregan genes, it appears that the aggregans were downregulated on the microfibrous scaffold (Fig. 6).

Discussion

The present study was designed to demonstrate the feasibility of hMSCs to maintain viability, orientation, and proliferation when cultured for 35 days on aligned electrospun nano- and microfibrous PCL scaffolds. Viable and aligned hMSCs were also cultured in media containing TGF-β_1 and induced to chondrogenically differentiate on the nano- and microfibrous scaffolds. Results indicate that hMSCs were able to maintain cell alignment on both types of fibrous PCL scaffolds, but chondrogenically differentiated to a greater extent when cultured on the nanofibrous scaffold. For example, hMSCs cultured in the chondrogenic differentiation media and seeded on the nanofibrous scaffold produced the highest levels of sGAG and mRNA specific to collagen type II and aggrecan. The level of collagen type II from nanofibrous scaffolds far exceeded any levels measured from the other scaffold types. This may indicate that such oriented nanofibrous PCL scaffolds may be better suited for engineering the superficial zone of articular cartilage, which naturally has a high content of collagen type II ECM compared to other cartilage zones.

We have recently demonstrated that an oriented nanofibrous scaffold can be used to guide cell alignment along the nanofibers.[22] Aligned cells could be then used to remodel and modulate the regenerated ECM and microenvironment.[23] The cell arrangement onto an oriented nanofibrous scaffold could be due to contact guidance and/or cytoskeletal reorganization. It has been previously shown that cell elongation induced by the aligned PCL nanofibers is expected to reorganize the cytoskeletal structures that regulate the cell morphology, adhesion, and locomotion.[24] Unlike microfilaments found in typical spread hMSCs on 2D substrates that can be described as large actin stress fibers and terminate at focal contact sites on the cell membrane,[25,26] hMSCs cultured on

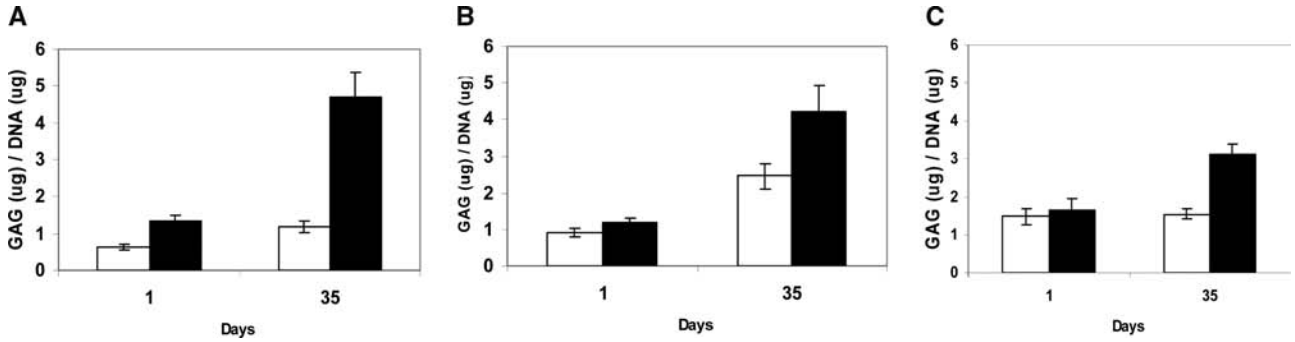

FIG. 5. Normalized sGAG content measurement at days 1 and 35. hMSCs cultured either in growth media (open bars) or in chondrogenic differentiation media (black bars) on electrospun oriented PCL fibrous scaffolds having average fiber diameters of 500 nm (**A**) and 3000 nm (**B**), as well as on nonelectrospun PCL film (**C**). Results represent the mean ± SEM of three independent experiments.

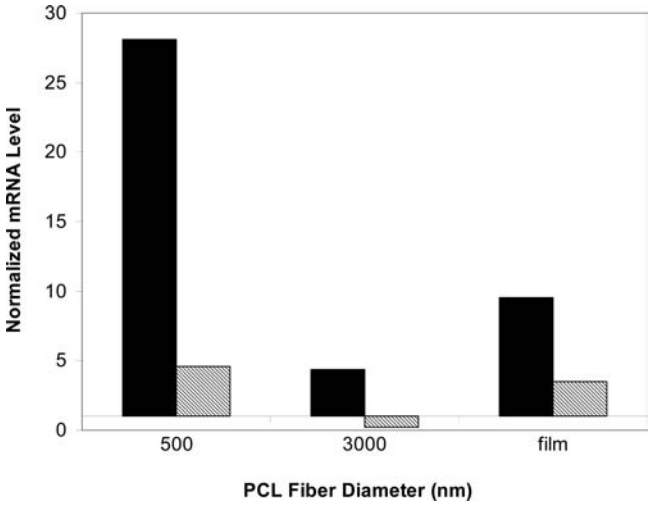

FIG. 6. PCR analysis of gene expressions for chondrogenic markers. The collagen type II gene (black bars) and aggregan gene (hatched bars) expression was measured from cells cultured in the chondrogenic differentiation media for 35 days on the nano- or microfibrous scaffolds and PCL film. GAPDH was used as a housekeeping control. The comparative CT method was used to show the fold-increases of the PCR results from samples cultured for 35 days in the chondrogenic differentiation media to those at day 1.

aligned PCL scaffolds showed much different actin cytoskeletal organization. For example, hMSCs seeded on the random nanofibrous scaffolds and cultured in hMSC growth media for 4 days displayed elongated cell morphologies and densely concentrated actins, and some actin filament bundles were predominantly aligned in the same direction as the adjacent nanofibers (Fig. 7; see Ref. 22). In addition, thin fibrous tether-like actin structures connecting the hMSC with the neighboring aligned nanofiber bundle were also observed. Unlike the membrane tethers (devoid of actins) formed by attaching a microbead to the cell membrane and pulling it away from the cell body,[25,26] these thin fibrous structures contain actins and likely adhesion proteins. Although it remains to be further studied, these findings could lead to the notion of unique hMSC binding characteristics to the nanofibers that may influence not only cell alignment but also improved cell differentiation (Figs. 5 and 6). We are currently examining these unique structures to test for the presence of focal adhesion proteins such as integrins and other intracellular proteins.

Our results are consistent with a previous report that vascular smooth muscle cells cultured on aligned polymeric nanofibrous scaffolds also develop similar fibrous connections.[14] It should be noted, however, that the images reported therein providing evidence of possible cell–nanofiber adhesions were obtained using SEM. In contrast, our findings show that not only similar fibrous connections are found in the hMSC–nanofiber interactions, but also actin filaments are likely involved in the development of these unique adhesion-like structures. It is also interesting to note that the dense actin networks observed in the elongated hMSCs cultured on oriented nanofibrous scaffolds appear similar to the cytoskeleton observed in mature articular chondrocytes, especially at the articular surface,[27] suggesting that the use of oriented nanofibrous polymeric scaffolds could be advantageous to better mimic articular cartilage tissue.[28–31]

In order to function properly, cells seeded in a scaffold must be able to communicate with their environment via appropriate biochemical, bioelectrical, and topological signals. The topography and composition of the microenvironment (i.e., native ECM) affect cellular functions, such as adhesion, morphology, proliferation, motility, gene expression, and apoptosis. It is well known that the physical

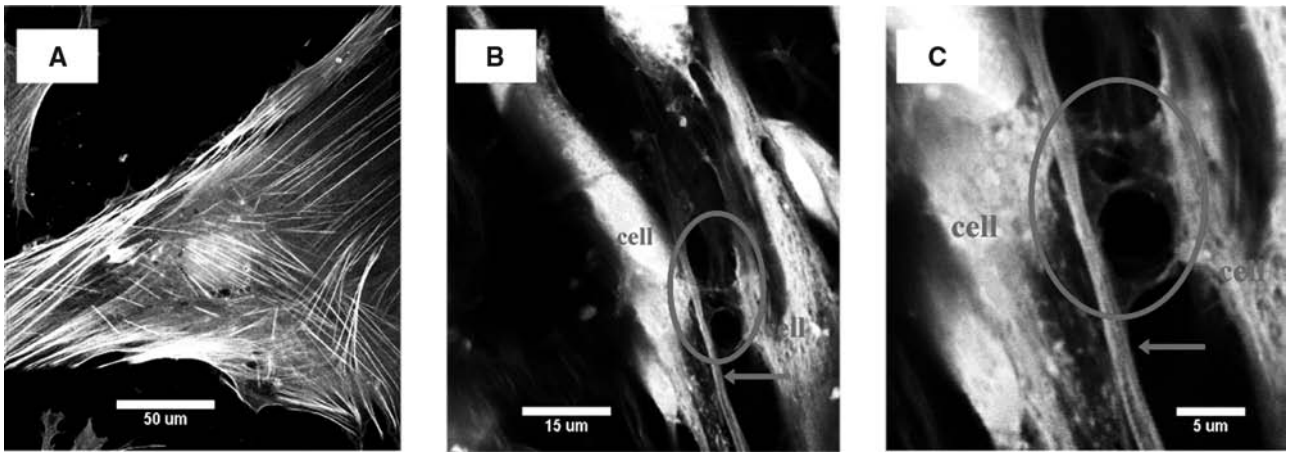

FIG. 7. Fluorescent images of reorganized microfilaments. Following 4 days of cell culture on a nanofibrous scaffold, microfilaments were visualized using rhodamine-phalloidine. Cells seeded on a typical culture dish demonstrate a spread cellular morphology and formation of thick bundle of stress fibers (**A**). In contrast, cells seeded on the nanofibrous PCL scaffold exhibit an elongated cellular morphology, as expected. Moreover, stress microfilament bundles were much less pronounced, but instead regions of concentrated actins were clearly seen (**B**). The actin-containing tether-like adhesions between cells and fibers (circled region) were observed only when the cells were cultured on the nanofibrous scaffold, and therefore appear to be unique for cell adhesion to nanofibers. Because the PCL fibers were imaged using reflection mode, distinction between fluorescently labeled microfilaments and nanofibers may not be obvious in this composite image. An arrow was drawn in the image to indicate the location of a PCL nanofiber. A magnified image (**C**) better illustrates the cell attachment to a nanofiber through a tether-like adhesion mechanism that utilizes F-actins.

structure of native ECM has nanoscale dimensions. The high surface-to-volume ratio of polymer nanofibrous scaffolds and the nanoscale diameter of the fibers, which mimic natural ECM matrix such as collagen fibrils, are likely to provide optimal conditions for cell attachment and growth. Indeed many types of cells have been shown to attach to and organize around fibers with diameters smaller than those of the cells, due to interaction of nanoscale cell membrane receptors such as integrins with the nanofibers.[32–34] Considering the diameter of the fibers produced by electrospinning for tissue engineering applications, it has been shown by others that endothelial cells adhered and proliferated markedly better on polymer nanofibers (300–1200 nm) than on microfibers (7 μm),[35] and that polymer nanofibers (500–900 nm) promote and regulate specifically the chondrocyte phenotype more efficiently than microfibers (15–20 μm).[31] Nanofibrous scaffolds produced by electrospinning biocompatible polymers, especially with controlled orientation, may also be ideal for engineering many specific types of tissues.[36,37] Macroscopically, the thin tissue-like constructs engineered in this study resembled the superficial zone of articular (hyaline) cartilage tissue and were generally mechanically strong for handling. Characterization of the mechanical properties of these thin electrospun nanofibrous PCL scaffolds is currently underway. We note that the elastic modulus of a single electrospun polymeric nanofiber can be as high as 1 GPa,[38,39] and that oriented polymeric nanofibrous scaffolds have mechanical properties in the MPa range, similar to native soft orthopedic tissues.[40] In addition, a nano tensile tester has been applied to measure the tensile strength of electrospun fibers (40 MPa for 1.4 μm diameter).[38] It is interesting to note that this mechanical property decreased with increasing fiber diameter. We also note that seeding cells on these PCL fibers is not expected to significantly alter their mechanical properties.

Characterization of mechanical properties is indeed important for assessing the functionality of any engineered tissue constructs. However, the aim of this work is to demonstrate the feasibility of engineering the superficial zone of articular cartilage by matching cell shape and alignment. Building upon this work, engineering a more functional articular cartilage tissue using a layer-by-layer approach in which the aligned superficial zone could be integrated with the middle zone and radial zone now appears feasible.

Conclusion

In the present study, we have successfully cultured hMSCs on oriented nano- and microfibrous electrospun PCL scaffolds as well as a random porous PCL film in either growth media or chondrogenic differentiation media, and quantitatively measured the cell orientation and proliferation, and chondrogenic markers. Taken together, our findings suggest that engineering an oriented ECM environment to regulate tissue alignment could be optimized by oriented electrospun nanofibers, and that specific tissue engineering applications, such as creating the superficial zone of articular cartilage, may be significantly improved by a combination of stem cells and nanofibrous scaffolds. Finally, additional experiments are currently underway to elucidate with molecular details the apparent cell adhesion mechanism(s) between hMSCs and nanofibers (Fig. 7) that could potentially play an important role in nanofiber-mediated stem cell differentiation. The hMSC adhesion on 2D substrates,[41] or in 3D collagen scaffolds[42] has been shown to be much different than that of terminally differentiated cells (e.g., osteoblasts). We note that differential adhesion to nanoscale features has also been observed and reported elsewhere. For example, both fibroblasts and osteoblasts exhibited decreased proliferation when cultured on substrates with nanofeatures and suppressed formation of actin network.[43,44] While our findings are consistent with the lack of actin fibers in cells cultured on nanotopographical features, hMSCs do not exhibit significant decrease in proliferation when cultured on the PCL fibers (Fig. 4), however. We postulate that the differential formation of cell type–dependent focal adhesion is likely to regulate stem cell behaviors in the nanoenvironment, including chondrogenic differentiation.

Acknowledgments

The authors are grateful to Dr. Igor Titushkin for his expertise and invaluable assistance with laser scanning confocal microscopy and image analysis, and to Nicole Green and Winnie Kuo for assistance with hMSC orientation and chondrogenic differentiation analysis. We also thank Kristina Jarosius of the UIC Research Resources Center for SEM experiments. This work was supported, in part, by NIH Grants (GM60741, EB06067, MC) and a grant from the Office of Naval Research (N00014-06-1-0100, MC). The production of the electrospun fibrous PCL scaffolds was supported by the Volkswagen Foundation (AY). Human mesenchymal stem cells used in this work were provided by the Tulane Center for Gene Therapy through an NIH grant (P40RR017447).

References

1. Hunziker, E.B. Articular cartilage structure in humans and experimental animals. In: Kuettner *et al.*, eds. Articular Cartilage and Osteoarthritis. New York: Raven Press, 1992, pp. 183–199.
2. Temenoff, J.S., and Mikos, A.G. Review: tissue engineering for regeneration of articular cartilage. Biomaterials **21,** 431, 2000.
3. Poole, A.R., Kojima, T., Yasuda, T., Mwale, F., Kobayashi, M., and Laverty, S. Composition and structure of articular cartilage: a template for tissue repair. Clin Orthop Relat Res **399 Suppl,** S26, 2001.
4. Jackson, D.W., Scheer, M.J., and Simon, T.M. Cartilage substitutes: overview of basic science and treatment options. J Am Acad Orthop Surg **9,** 37, 2001.
5. Hunziker, E.B., Quinn, T.M., and Haeuselmann, H.-J. Quantitative structural organization of normal adult human articular cartilage. Osteoarthritis Cartilage **10,** 564, 2002.
6. Poole, A.R. What type of cartilage repair are we attempting to attain? J Bone Joint Surg **85,** 40, 2003.
7. Eyre, D. Collagen of articular cartilage. Arthritis Res **4,** 30, 2002.
8. Setton, L.A., Elliott, D.M., and Mow, V.C. Altered mechanics of cartilage with osteoarthritis: human osteoarthritis and an experimental model of joint degeneration. Osteoarthritis Cartilage **7,** 2, 1999.
9. Mow, V.C. and Guo, X.E. Mechano-electrochemical properties of articular cartilage: their inhomogeneities and anisotropies. Annu Rev Biomed Eng **4,** 175, 2002.
10. Sah, R.L. The biomechanical faces of articular cartilage. In: Kuettner, K.E., and Hascall, V.C., eds. The Many Faces of Osteoarthritis. New York: Raven Press, 2002, pp. 409–422.

11. Wong, M., and Carter, D.R. Articular cartilage functional histomorphology and mechanobiology: a research perspective. Bone **33,** 1, 2003.
12. Guilak, F., Butler, D.L., Goldstein, S.A., and Mooney, D.J., eds. Functional Tissue Engineering. New York: Springer-Verlag, 2003; pp. 46–68, 227–242, 277–290.
13. Owen, J.R., and Wayne, J.S. Influence of a superficial tangential zone over repairing cartilage defects: implications for tissue engineering. Biomech Model Mechanobiol **5,** 102, 2006.
14. Xu, C.Y., Inai, R., Kotaki, M., and Ramakrishna, S. Aligned biodegradable nanofibrous structure: a potential scaffold for blood vessel engineering. Biomaterials **25,** 877, 2004.
15. Yang, F., Murugan, R., Wang, S., and Ramakrishna, S. Electrospinning of nano/micro scale poly(L-lactic acid) aligned fibers and their potential in neural tissue engineering. Biomaterials **26,** 2603, 2005.
16. Lee, C.H., Shin, H.J., Cho, I.H., Kang, Y.M., Kim, I.A., Park, K.D., and Shin, J.W. Nanofiber alignment and direction of mechanical strain affect the ECM production of human ACL fibroblast. Biomaterials **26,** 1261, 2005.
17. Li, W.-J., Mauck, R.L., Cooper, J.A., Yuan, X., and Tuan, R.S. Engineering controllable anisotropy in electrospun biodegradable nanofibrous scaffolds for musculoskeletal tissue engineering. J Biomech **40,** 1686, 2007.
18. Baker, B.M., and Mauck, R.L. The effect of nanofiber alignment on the maturation of engineered meniscus constructs. Biomaterials **28,** 1967, 2007.
19. Reneker, D.H., Yarin, A.L., Fong, H., and Koombhongse, S. Bending instability of electrically charged liquid jets of polymer solutions in electrospinning. J Appl Phys **87,** 4531, 2000.
20. Theron, A., Zussman, E., and Yarin, A.L. Electrostatic field-assisted alignment of electrospun nanofibres. Nanotechnology **12,** 384, 2001.
21. Zussman, E., Theron, A., and Yarin, A.L. Formation of nanofiber crossbars in electrospinning. Appl Phys Lett **82,** 973, 2003.
22. Wise, J.K., Cho, M.R., Zussman, E., Megaridis, C.M., and Yarin, A.L. Electrospinning techniques to control deposition and structural alignment of nanofibrous scaffolds for cellular orientation and cytoskeletal reorganization. In: Laurencin, C., and Nair, L.S. ed. Nanotechnology and Tissue Engineering: The Scaffold. CRC Press, 2008. pp. 243–260.
23. Wang, J.H.-C., Jia, F., Gilbert, T.W., and Woo, S.L.-Y. Cell orientation determines the alignment of cell-produced collagenous matrix. J Biomech **36,** 97, 2003.
24. Dunn, G.A. Contact guidance of cultured tissue cells: a survey of potentially relevant properties of the substratum. In: Bellairs, R., Curtis, A., and Dunn, G., eds. Cell Behaviour. Cambridge: Cambridge University Press, 1982, pp. 247–280.
25. Titushkin, I., and Cho, M. Modulation of cellular mechanics during osteogenic differentiation of human mesenchymal stem cells. Biophys J **93,** 3693, 2007.
26. Chen, H., Titushkin, I., Stroscio, M., and Cho, M. Altered membrane dynamics of quantum dot-conjugated integrins during osteogenic differentiation of human bone marrow derived progenitor cells. Biophys J **92,** 1399, 2007.
27. Langelier, E., Suetterlin, R., Hoemann, C.D., Aebi, U., and Buschmann, M.D. The chondrocyte cytoskeleton in mature articular cartilage: structure and distribution of actin, tubulin, and vimentin filaments. J Histochem Cytochem **48,** 1307, 2000.
28. Li, W.-J., Danielson, K.G., Alexander, P.G., and Tuan, R.S. Biological response of chondrocytes cultured in three-dimensional nanofibrous poly(epsilon-caprolactone) scaffolds. J Biomed Mater Res **67A,** 1105, 2003.
29. Li, W.-J., Tuli, R., Okafor, C., Derfoul, A., Danielson, K.G., Hall, D.J., and Tuan, R.S. A three-dimensional nanofibrous scaffold for cartilage tissue engineering using human mesenchymal stem cells. Biomaterials **26,** 599, 2005.
30. Li, W.-J., Tuli, R., Huang, X., Laquerriere, P., and Tuan, R.S. Multilineage differentiation of human mesenchymal stem cells in a three-dimensional nanofibrous scaffold. Biomaterials **26,** 5158, 2005.
31. Li, W.-J., Jiang, Y.-J., and Tuan, R.S. Chondrocyte phenotype in engineered fibrous matrix is regulated by fiber size. Tissue Eng **12,** 1, 2006.
32. Laurencin, C.T., Ambrosio, A.M., Borden, M.D., and Cooper, J.J. Tissue engineering: orthopedic applications. Annu Rev Biomed Eng **1,** 19, 1999.
33. Ma, Z., Kotaki, M., Inai, R., and Ramakrishna, S. Potential of nanofiber matrix as tissue-engineering scaffolds. Tissue Eng **11,** 101, 2005.
34. Toh, Y.-C., Ng, S., Khong, Y.M., Zhang, X., Zhu, Y., Lin, P.C., Te, C.-M., Sun, W., and Yu, H. Cellular responses to a nanofibrous environment. Nano Today **1,** 34, 2006.
35. Kwon, I.-K., Kidoaki, S., and Matsuda, T. Electrospun nano- to microfiber fabrics made of biodegradable copolyesters: structural characteristics, mechanical properties and cell adhesion potential. Biomaterials **26,** 3929, 2005.
36. Murugan, R., and Ramakrishna, S. Design strategies of tissue engineering scaffolds with controlled fiber orientation. Tissue Eng **13,** 1845, 2007.
37. Ashammakhi, N., Ndreu, A., Yang, Y., Ylikauppila, H., Nikkola, L., and Hasirci, V. Tissue engineering: a new take-off using nanofiber-based scaffolds. J Craniofac Surg **18,** 3, 2007.
38. Tan, E.P.S., and Lim, C.T. Physical properties of a single polymeric nanofiber. Appl Phys Lett **84,** 1603, 2004.
39. Zussman, E., Burman, M., Yarin, A.L., Khalfin, R., and Cohen, Y. Tensile deformation of electrospun Nylon 6,6 nanofibers. J Polym Sci Part B-Polym Phys **44,** 1482, 2006.
40. Nerurkar, N.L., Elliot, D.M., and Mauck, R.L. Mechanics of oriented electrospun nanofibrous scaffolds for annulus fibrosus tissue engineering. J Orthop Res **25,** 1018, 2007.
41. Titushkin, I.A., and Cho, M. Regulation of cell cytoskeleton and membrane mechanics by electric field: role of linker proteins. Biophys J Manuscript in revision.
42. Sun, S., Titushkin, I.A., and Cho, M. Regulation of mesenchymal stem cell adhesion and orientation in 3D collagen scaffold by electrical stimulus. Bioelectrochemistry **69,** 133, 2006.
43. Kunzler, T.P., Huwilen, C., Tanja, D., Janos, V., and Spencer, N. Systematic study of osteoblast response to nanotopography by means of nanoparticle-density gradients. Biomaterials **28,** 2175, 2007.
44. Dalby, M.J., Riehle, M., Johnstone, H.J.H., Affrossman, S., and Curtis, A.S. Polymer-demixing nanotopography: control of fibroblast spreading and proliferation. Tissue Eng **8,** 1099, 2002.

Address reprint requests to:
Michael Cho, Ph.D.
Department of Bioengineering
University of Illinois at Chicago
851 S. Morgan St. (M/C 063)
Chicago, IL 60607

E-mail: mcho@uic.edu

Received: February 15, 2008
Accepted: June 20, 2008
Online Publication Date: August 29, 2008